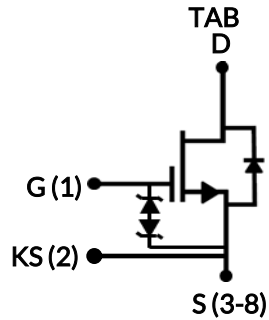
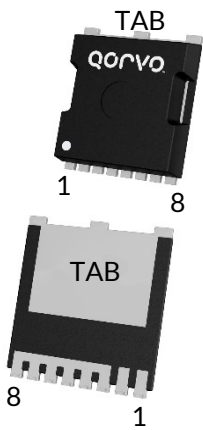


DATASHEET

UJ4SC075005L8S



750V-5.4mΩ SiC FET

Rev. A, February 2023

Description

The UJ4SC075005L8S is a 750V, 5.4mΩ G4 SiC FET. It is based on a unique ‘cascode’ circuit configuration, in which a normally-on SiC JFET is co-packaged with a Si MOSFET to produce a normally-off SiC FET device. The device’s standard gate-drive characteristics allows use of off-the-shelf gate drivers hence requiring minimal re-design when replacing Si IGBTs, Si superjunction devices or SiC MOSFETs. Available in the space-saving MO-229 package which enables automated assembly, this device exhibits ultra-low gate charge and exceptional reverse recovery characteristics, making it ideal for switching inductive loads and any application requiring standard gate drive.

Features

- ◆ On-resistance $R_{DS(on)}$: 5.4mΩ (typ)
- ◆ Operating temperature: 175°C (max)
- ◆ Excellent reverse recovery: Q_{rr} = 440nC
- ◆ Low body diode V_{FSD} : 1.03V
- ◆ Low gate charge: Q_G = 164nC
- ◆ Threshold voltage $V_{G(th)}$: 4.7V (typ) allowing 0 to 15V drive
- ◆ Low intrinsic capacitance
- ◆ ESD protected, HBM class 2
- ◆ MO-229 package for faster switching, clean gate waveforms

Typical applications

- ◆ Solid state relays and circuit-breakers
- ◆ Line rectification and active-bridge rectification circuits in AC/DC front-ends
- ◆ EV charging
- ◆ PV inverters
- ◆ Switch mode power supplies
- ◆ Power factor correction modules
- ◆ Motor drives
- ◆ Induction heating

| Part Number | Package | Marking |
|----------------|---------|-------------|
| UJ4SC075005L8S | MO-229 | UJ4SC075005 |



Maximum Ratings

| Parameter | Symbol | Test Conditions | Value | Units |
|---|----------------|--|------------|------------------|
| Drain-source voltage | V_{DS} | | 750 | V |
| Gate-source voltage | V_{GS} | DC | -20 to +20 | V |
| | | AC (f > 1Hz) | -25 to +25 | V |
| Continuous drain current ¹ | I_D | $T_C < 144^\circ\text{C}$ | 120 | A |
| Pulsed drain current ² | I_{DM} | $T_C = 25^\circ\text{C}$ | 588 | A |
| Single pulsed avalanche energy ³ | E_{AS} | L=15mH, $I_{AS} = 6.5\text{A}$ | 316 | mJ |
| Short circuit withstand time ⁴ | t_{SC} | $V_{DS} = 400\text{V}$, $T_{J(\text{START})} = 175^\circ\text{C}$ | 5 | μs |
| SiC FET dv/dt ruggedness | dv/dt | $V_{DS} \leq 500\text{V}$ | 100 | V/ns |
| Power dissipation | P_{tot} | $T_C = 25^\circ\text{C}$ | 1153 | W |
| Maximum junction temperature | $T_{J,max}$ | | 175 | $^\circ\text{C}$ |
| Operating and storage temperature | T_J, T_{STG} | | -55 to 175 | $^\circ\text{C}$ |
| Reflow soldering temperature | T_{solder} | reflow MSL 1 | 260 | $^\circ\text{C}$ |

- Limited by bondwires
- Pulse width t_p limited by $T_{J,max}$
- Starting $T_J = 25^\circ\text{C}$
- Short circuit current is independent of the gate voltage $V_{GS} > 12\text{V}$

Thermal Characteristics

| Parameter | Symbol | Test Conditions | Value | | | Units |
|--------------------------------------|-----------------|-----------------|-------|------|------|--------------------|
| | | | Min | Typ | Max | |
| Thermal resistance, junction-to-case | $R_{\theta JC}$ | | | 0.10 | 0.13 | $^\circ\text{C/W}$ |

Electrical Characteristics ($T_J = +25^\circ\text{C}$ unless otherwise specified)

Typical Performance - Static

| Parameter | Symbol | Test Conditions | Value | | | Units |
|--------------------------------|--------------|---|-------|------|-----|---------------|
| | | | Min | Typ | Max | |
| Drain-source breakdown voltage | BV_{DS} | $V_{GS}=0V, I_D=1mA$ | 750 | | | V |
| Total drain leakage current | I_{DSS} | $V_{DS}=750V, V_{GS}=0V, T_J=25^\circ\text{C}$ | | 6 | 130 | μA |
| | | $V_{DS}=750V, V_{GS}=0V, T_J=175^\circ\text{C}$ | | 45 | | |
| Total gate leakage current | I_{GSS} | $V_{DS}=0V, T_J=25^\circ\text{C}, V_{GS}=-20V / +20V$ | | 6 | 20 | μA |
| Drain-source on-resistance | $R_{DS(on)}$ | $V_{GS}=12V, I_D=80A, T_J=25^\circ\text{C}$ | | 5.4 | 7.2 | m Ω |
| | | $V_{GS}=12V, I_D=80A, T_J=125^\circ\text{C}$ | | 9.3 | | |
| | | $V_{GS}=12V, I_D=80A, T_J=175^\circ\text{C}$ | | 12.2 | | |
| Gate threshold voltage | $V_{G(th)}$ | $V_{DS}=5V, I_D=10mA$ | 4 | 4.7 | 6 | V |
| Gate resistance | R_G | $f=1\text{MHz}, \text{open drain}$ | | 0.8 | 1.5 | Ω |

Typical Performance - Reverse Diode

| Parameter | Symbol | Test Conditions | Value | | | Units |
|---|---------------|--|-------|------|------|-------|
| | | | Min | Typ | Max | |
| Diode continuous forward current ¹ | I_S | $T_C < 144^\circ\text{C}$ | | | 120 | A |
| Diode pulse current ² | $I_{S,pulse}$ | $T_C=25^\circ\text{C}$ | | | 588 | A |
| Forward voltage | V_{FSD} | $V_{GS}=0V, I_S=50A, T_J=25^\circ\text{C}$ | | 1.03 | 1.16 | V |
| | | $V_{GS}=0V, I_S=50A, T_J=175^\circ\text{C}$ | | 1.06 | | |
| Reverse recovery charge | Q_{rr} | $V_{DS}=400V, I_S=80A, V_{GS}=0V, R_G=20\Omega$ | | 440 | | nC |
| Reverse recovery time | t_{rr} | $di/dt=2800A/\mu\text{s}, T_J=25^\circ\text{C}$ | | 31 | | ns |
| Reverse recovery charge | Q_{rr} | $V_{DS}=400V, I_S=80A, V_{GS}=0V, R_G=20\Omega$ | | 525 | | nC |
| Reverse recovery time | t_{rr} | $di/dt=2800A/\mu\text{s}, T_J=150^\circ\text{C}$ | | 37 | | ns |

Typical Performance - Dynamic

| Parameter | Symbol | Test Conditions | Value | | | Units | |
|--|---------------|--|--|------|------|---------|---------|
| | | | Min | Typ | Max | | |
| Input capacitance | C_{iss} | $V_{DS}=400V, V_{GS}=0V$ $f=100kHz$ | | 8374 | | pF | |
| Output capacitance | C_{oss} | | | 362 | | | |
| Reverse transfer capacitance | C_{rss} | | | 4 | | | |
| Effective output capacitance, energy related | $C_{oss(er)}$ | $V_{DS}=0V$ to 400V, $V_{GS}=0V$ | | 475 | | pF | |
| Effective output capacitance, time related | $C_{oss(tr)}$ | $V_{DS}=0V$ to 400V, $V_{GS}=0V$ | | 950 | | pF | |
| C_{OSS} stored energy | E_{oss} | $V_{DS}=400V, V_{GS}=0V$ | | 38 | | μJ | |
| Total gate charge | Q_G | $V_{DS}=400V, I_D=80A,$ $V_{GS} = 0V$ to 15V | | 164 | | nC | |
| Gate-drain charge | Q_{GD} | | | 24 | | | |
| Gate-source charge | Q_{GS} | | | 46 | | | |
| Turn-on delay time | $t_{d(on)}$ | Notes 5 and 6, $V_{DS}=400V, I_D=80A,$ Gate Driver =0V to +15V, Turn-on $R_{G,EXT}=1.5\Omega,$ Turn-off $R_{G,EXT}=5\Omega,$ inductive Load, FWD: same device with $V_{GS} = 0V$ and $R_G = 5\Omega,$ RC snubber: $R_S=5\Omega$ and $C_S=680pF,$ $T_J=25^\circ C$ | | 35 | | ns | |
| Rise time | t_r | | | 39 | | | |
| Turn-off delay time | $t_{d(off)}$ | | | 109 | | | |
| Fall time | t_f | | | 13 | | | |
| Turn-on energy including R_S energy | E_{ON} | | | | 766 | | μJ |
| Turn-off energy including R_S energy | E_{OFF} | | | | 162 | | |
| Total switching energy | E_{TOTAL} | | | | 928 | | |
| Snubber R_S energy during turn-on | E_{RS_ON} | | | | 17.6 | | |
| Snubber R_S energy during turn-off | E_{RS_OFF} | | | | 7.2 | | |
| Turn-on delay time | $t_{d(on)}$ | | Notes 5 and 6, $V_{DS}=400V, I_D=80A,$ Gate Driver =0V to +15V, Turn-on $R_{G,EXT}=1.5\Omega,$ Turn-off $R_{G,EXT}=5\Omega,$ inductive Load, FWD: same device with $V_{GS} = 0V$ and $R_G = 5\Omega,$ RC snubber: $R_S=5\Omega$ and $C_S=680pF,$ $T_J=150^\circ C$ | | 37 | | ns |
| Rise time | t_r | | | 41 | | | |
| Turn-off delay time | $t_{d(off)}$ | | | 114 | | | |
| Fall time | t_f | | | 13 | | | |
| Turn-on energy including R_S energy | E_{ON} | | | | 808 | | μJ |
| Turn-off energy including R_S energy | E_{OFF} | | | | 187 | | |
| Total switching energy | E_{TOTAL} | | | | 995 | | |
| Snubber R_S energy during turn-on | E_{RS_ON} | | | | 18.3 | | |
| Snubber R_S energy during turn-off | E_{RS_OFF} | | | | 10.3 | | |

5. Measured with the switching test circuit in Figure 26.

6. In this datasheet, all the switching energies (turn-on energy, turn-off energy and total energy) presented in the tables and Figures include the device RC snubber energy losses.

Typical Performance Diagrams

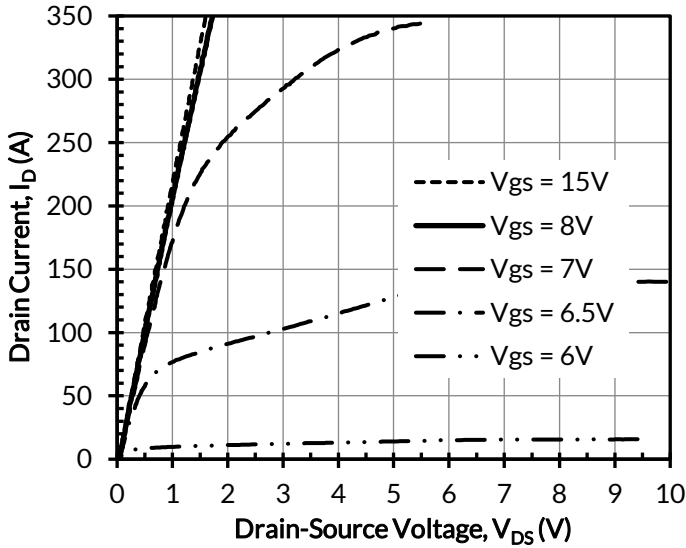


Figure 1. Typical output characteristics at $T_j = -55^\circ\text{C}$, $t_p < 250\mu\text{s}$

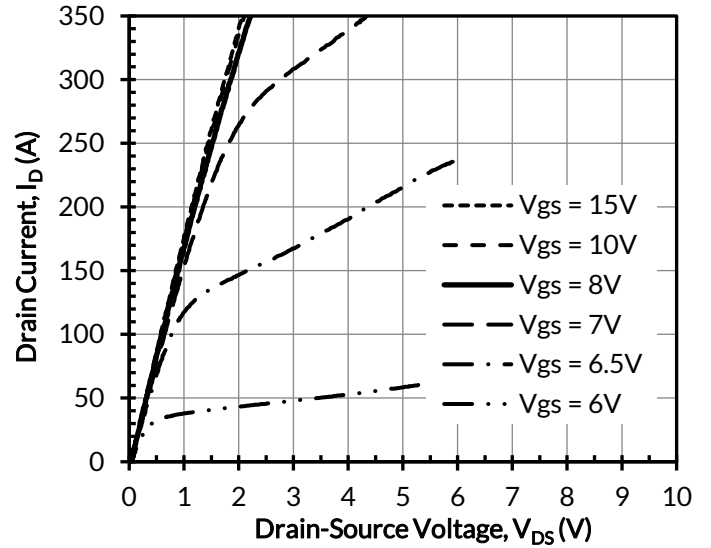


Figure 2. Typical output characteristics at $T_j = 25^\circ\text{C}$, $t_p < 250\mu\text{s}$

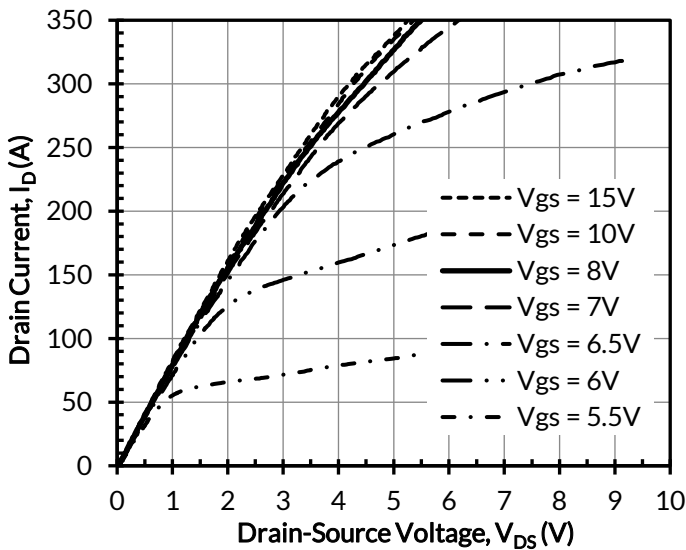


Figure 3. Typical output characteristics at $T_j = 175^\circ\text{C}$, $t_p < 250\mu\text{s}$

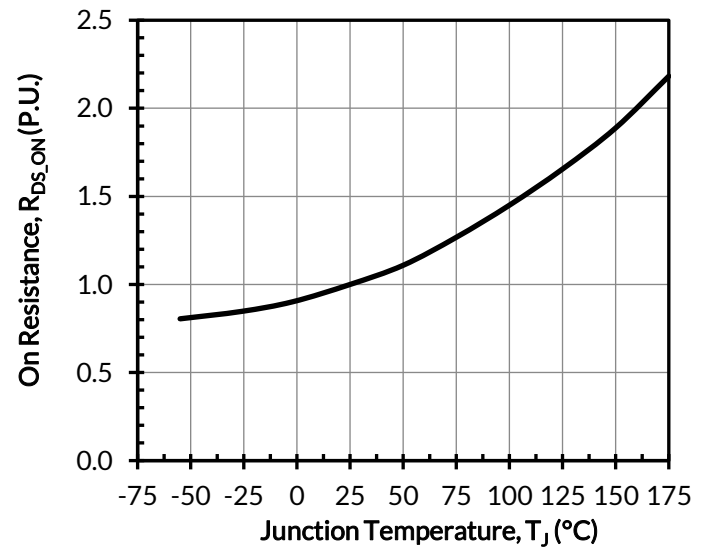


Figure 4. Normalized on-resistance vs. temperature at $V_{GS} = 12\text{V}$ and $I_D = 80\text{A}$

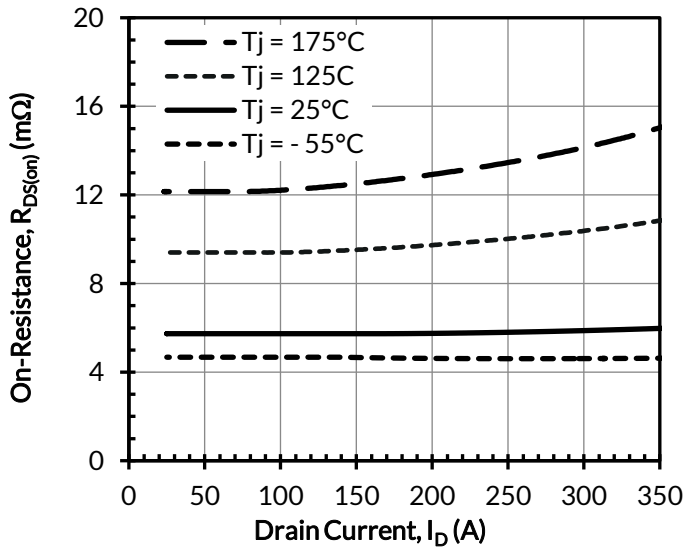


Figure 5. Typical drain-source on-resistances at $V_{GS} = 12V$

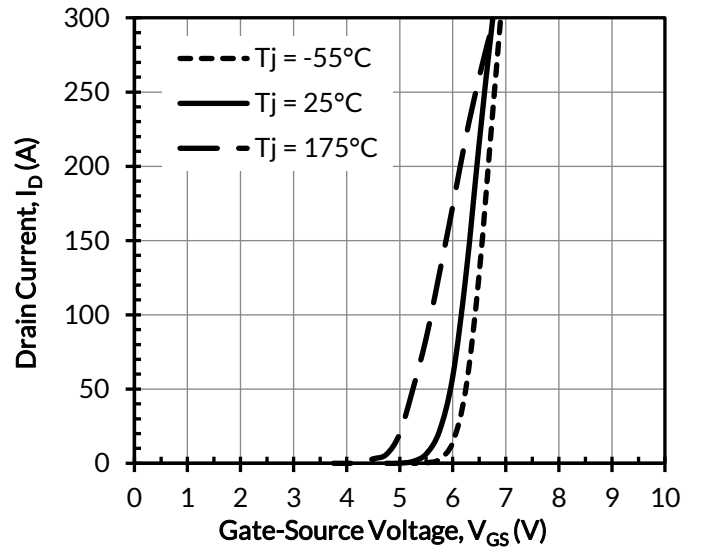


Figure 6. Typical transfer characteristics at $V_{DS} = 5V$

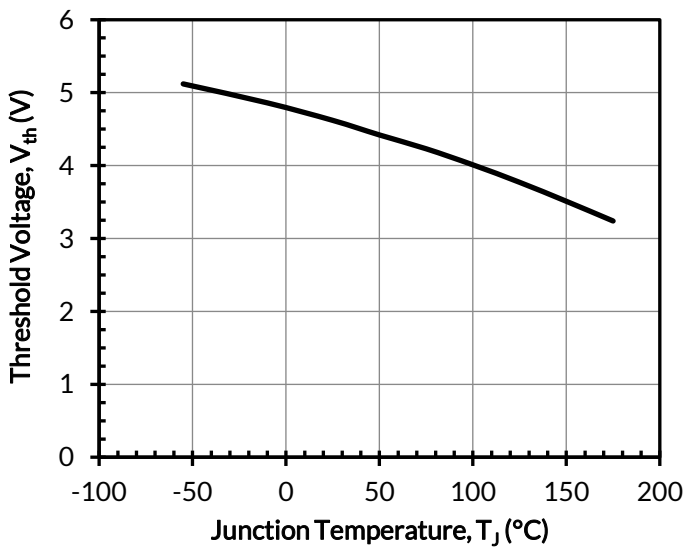


Figure 7. Threshold voltage vs. junction temperature at $V_{DS} = 5V$ and $I_D = 10mA$

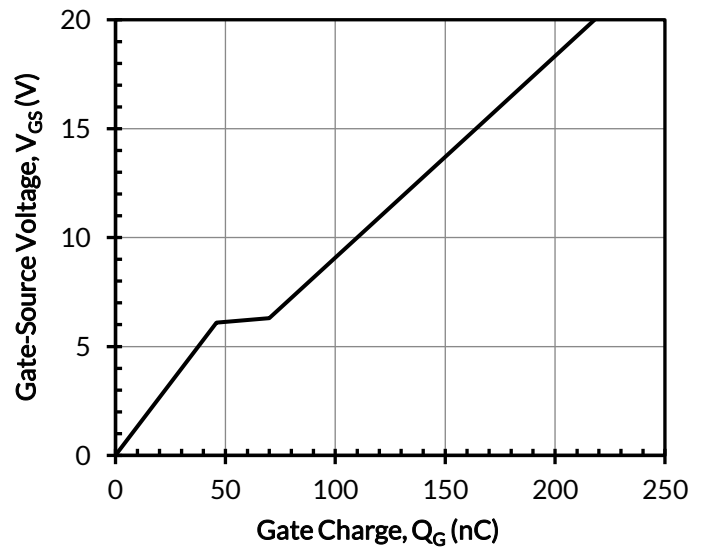


Figure 8. Typical gate charge at $V_{DS} = 400V$ and $I_D = 80A$

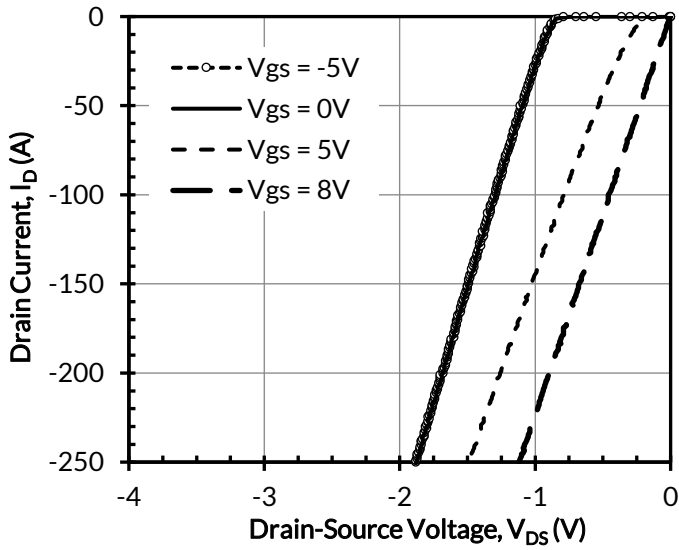


Figure 9. 3rd quadrant characteristics at $T_j = -55^\circ\text{C}$

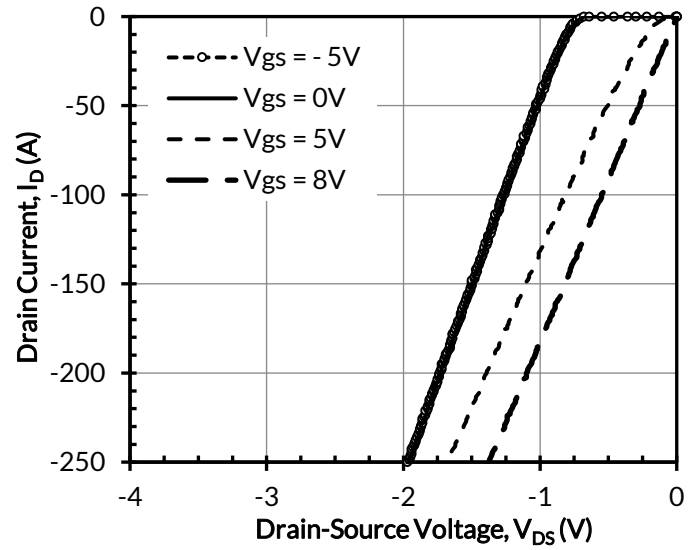


Figure 10. 3rd quadrant characteristics at $T_j = 25^\circ\text{C}$

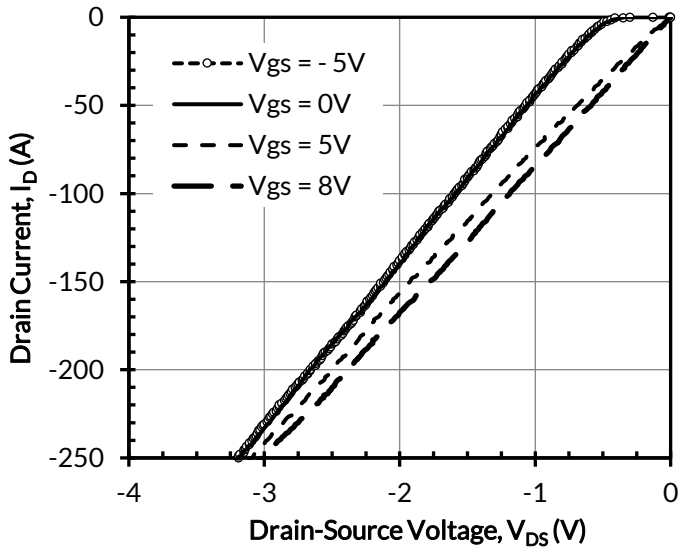


Figure 11. 3rd quadrant characteristics at $T_j = 175^\circ\text{C}$

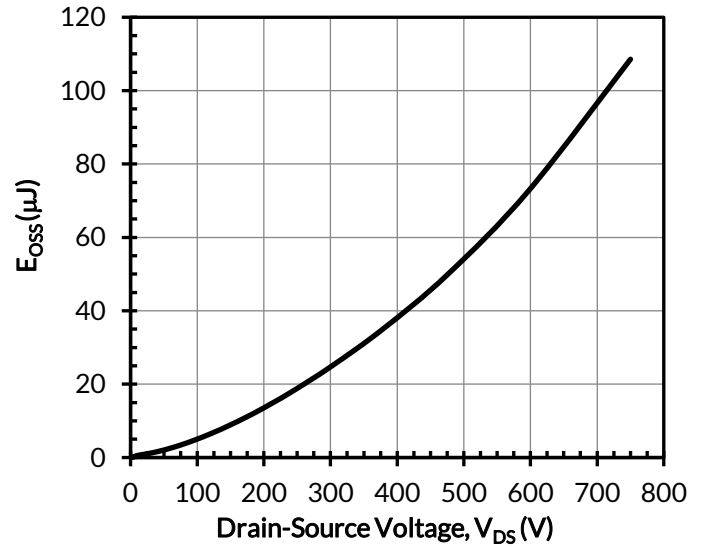


Figure 12. Typical stored energy in C_{OSS} at $V_{GS} = 0\text{V}$

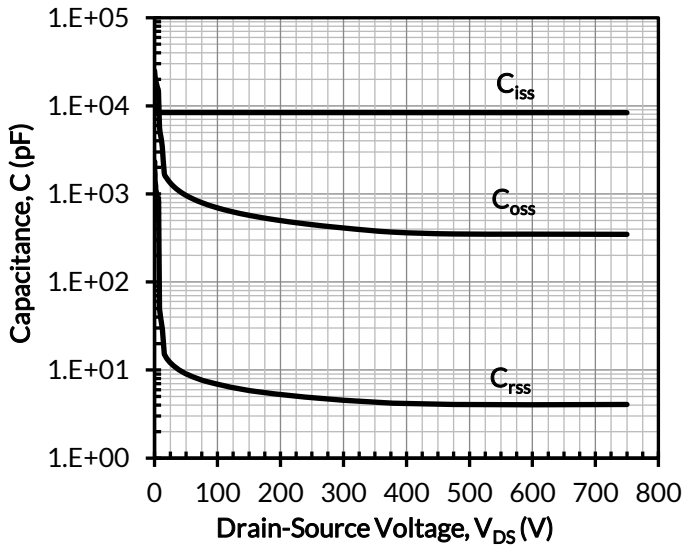


Figure 13. Typical capacitances at $f = 100\text{kHz}$ and $V_{GS} = 0\text{V}$

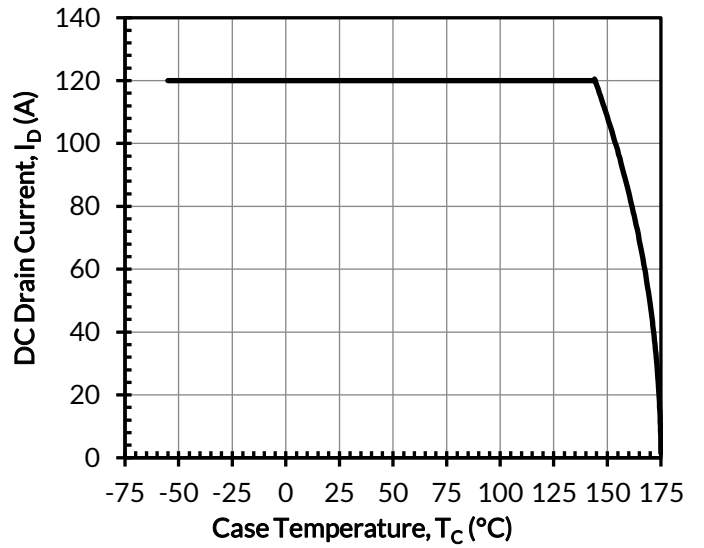


Figure 14. DC drain current derating

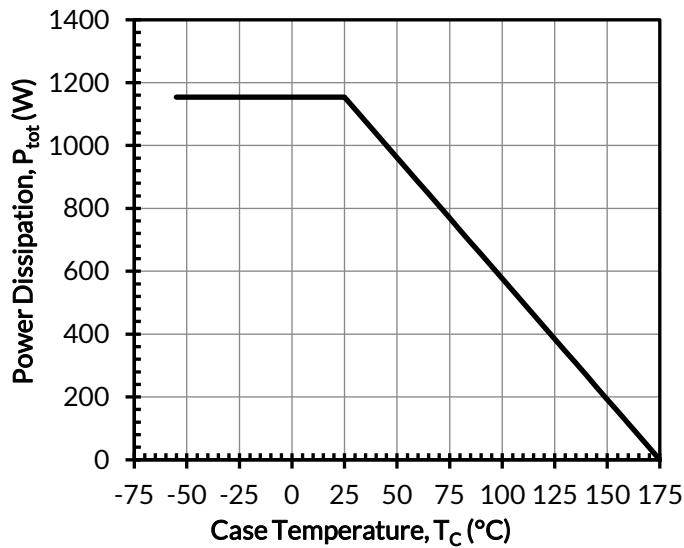


Figure 15. Total power dissipation

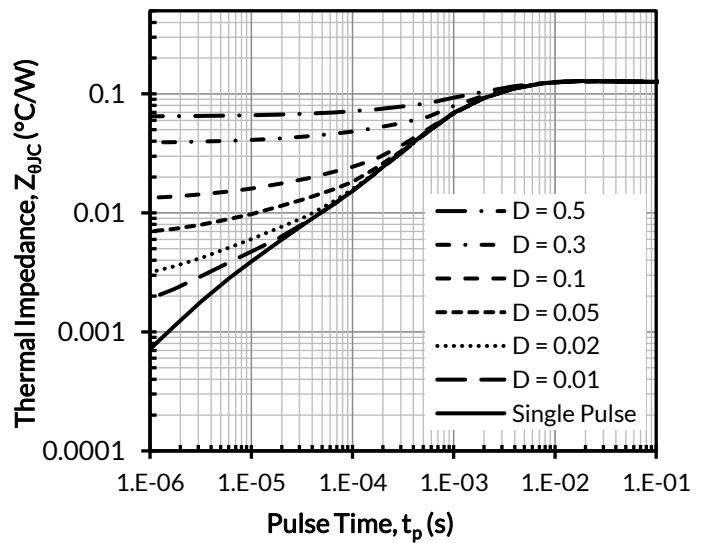


Figure 16. Maximum transient thermal impedance

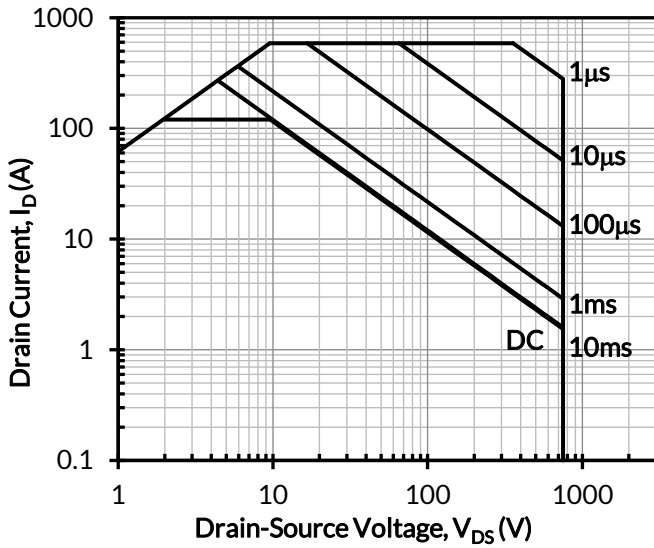


Figure 17. Safe operation area at $T_C = 25^\circ\text{C}$, $D = 0$, Parameter t_p

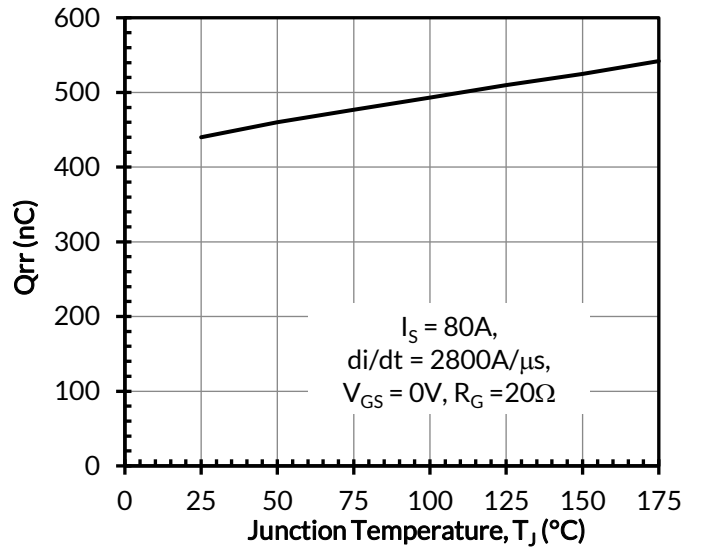


Figure 18. Reverse recovery charge Q_{rr} vs. junction temperature at $V_{DS} = 400\text{V}$

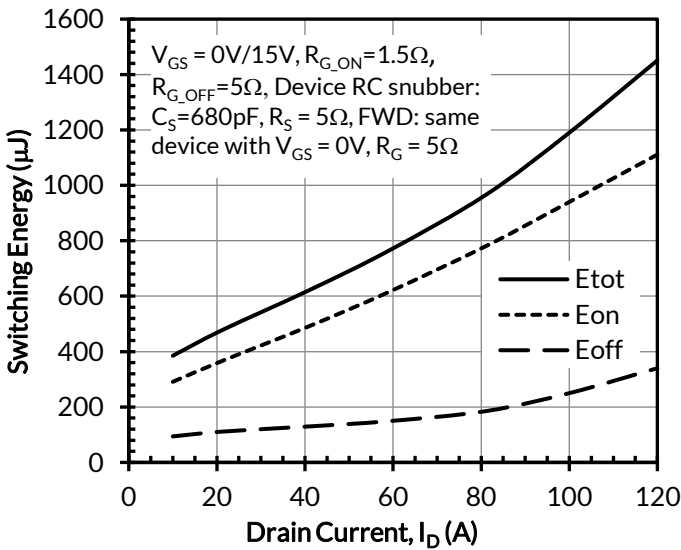


Figure 19. Clamped inductive switching energy vs. drain current at $V_{DS} = 400\text{V}$ and $T_J = 25^\circ\text{C}$

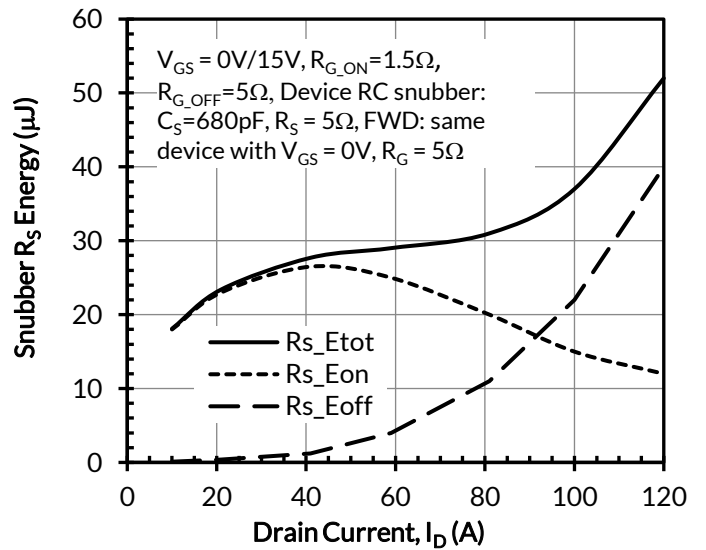


Figure 20. RC snubber energy loss vs. drain current at $V_{DS} = 400\text{V}$ and $T_J = 25^\circ\text{C}$

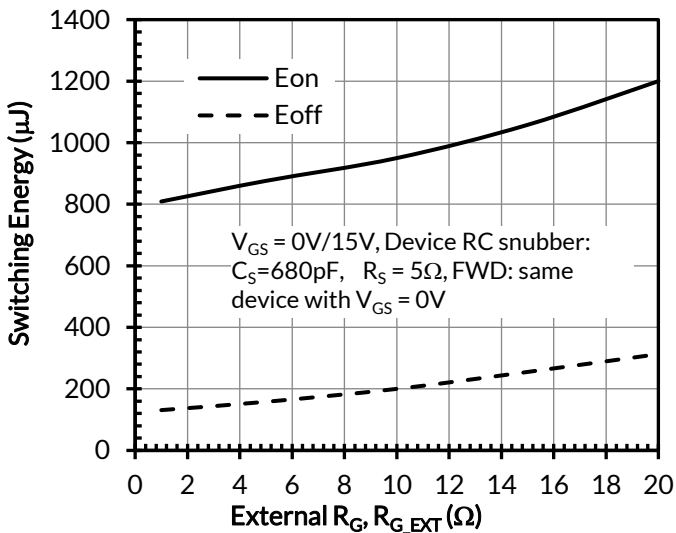


Figure 21. Clamped inductive switching energies vs. R_{G_EXT} at $V_{DS} = 400V$, $I_D = 80A$, and $T_J = 25^\circ C$

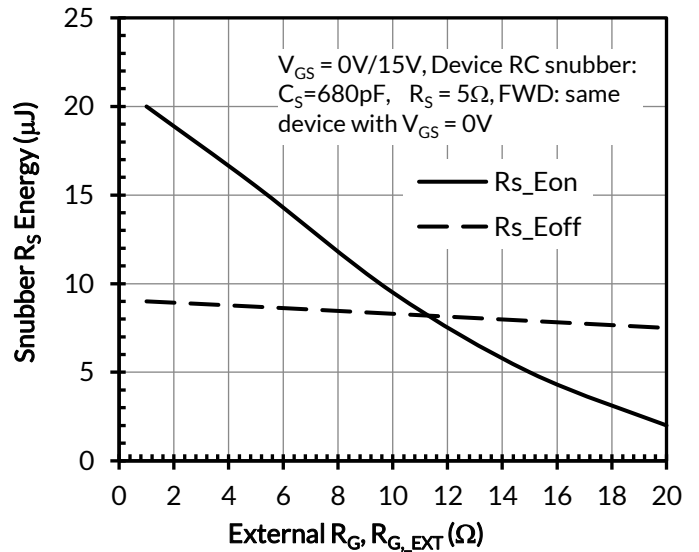


Figure 22. RC snubber energy losses vs. R_{G_EXT} at $V_{DS} = 400V$, $I_D = 80A$, and $T_J = 25^\circ C$

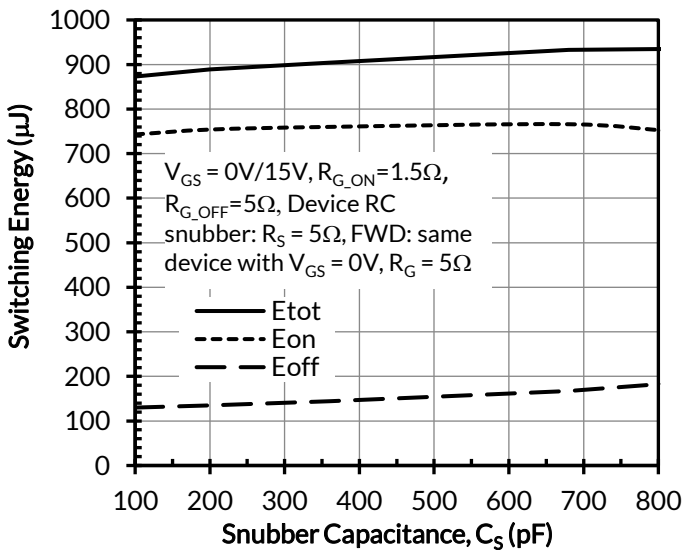


Figure 23. Clamped inductive switching energies vs. snubber capacitance C_S at $V_{DS} = 400V$, $I_D = 80A$, and $T_J = 25^\circ C$

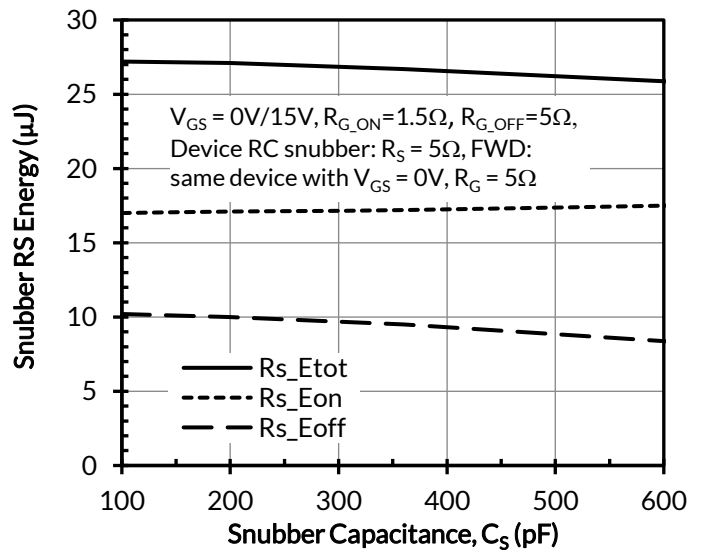


Figure 24. RC snubber energy losses vs. snubber capacitance C_S at $V_{DS} = 400V$, $I_D = 80A$, and $T_J = 25^\circ C$

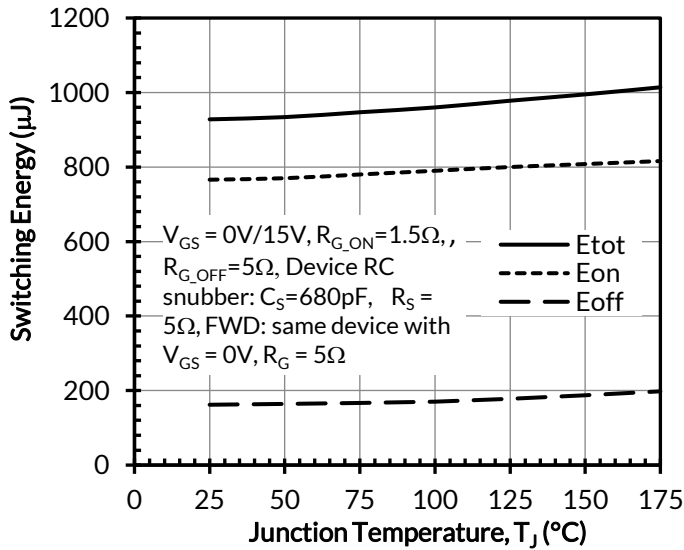


Figure 25. Clamped inductive switching energy vs. junction temperature at $V_{DS} = 400V$ and $I_D = 80A$

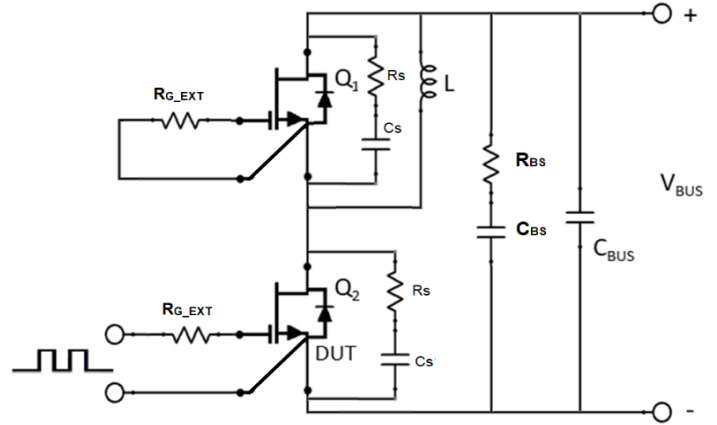


Figure 26. Schematic of the half-bridge mode switching test circuit. Note, a device snubber ($R_S = 5\Omega, C_S = 680pF$) and bus RC snubber ($R_{BS} = 1\Omega, C_{BS} = 100nF$) is used to reduce the power loop high frequency oscillations.

Applications Information

SiC FETs are enhancement-mode power switches formed by a high-voltage SiC depletion-mode JFET and a low-voltage silicon MOSFET connected in series. The silicon MOSFET serves as the control unit while the SiC JFET provides high voltage blocking in the off state. This combination of devices in a single package provides compatibility with standard gate drivers and offers superior performance in terms of low on-resistance ($R_{DS(on)}$), output capacitance (C_{oss}), gate charge (Q_G), and reverse recovery charge (Q_{rr}) leading to low conduction and switching losses. The SiC FETs also provide excellent reverse conduction capability eliminating the need for an external anti-parallel diode.

Like other high performance power switches, proper PCB layout design to minimize circuit parasitics is strongly recommended due to the high dv/dt and di/dt rates. An external gate resistor is recommended when the FET is working in the diode mode in order to achieve the optimum reverse recovery performance. For more information on SiC FET operation, see www.unitedsic.com.

A snubber circuit with a small $R_{(G)}$, or gate resistor, provides better EMI suppression with higher efficiency compared to using a high $R_{(G)}$ value. There is no extra gate delay time when using the snubber circuitry, and a small $R_{(G)}$ will better control both the turn-off $V_{(DS)}$ peak spike and ringing duration, while a high $R_{(G)}$ will damp the peak spike but result in a longer delay time. In addition, the total switching loss when using a snubber circuit is less than using high $R_{(G)}$, while greatly reducing $E_{(OFF)}$ from mid-to-full load range with only a small increase in $E_{(ON)}$. Efficiency will therefore improve with higher load current. For more information on how a snubber circuit will improve overall system performance, visit the UnitedSiC website at www.unitedsic.com

Important notice

The information contained herein is believed to be reliable; however, Qorvo makes no warranties regarding the information contained herein and assumes no responsibility or liability whatsoever for the use of the information contained herein. All information contained herein is subject to change without notice. Customers should obtain and verify the latest relevant information before placing orders for Qorvo products. The information contained herein or any use of such information does not grant, explicitly or implicitly, to any party any patent rights, licenses, or any other intellectual property rights, whether with regard to such information itself or anything described by such information. THIS INFORMATION DOES NOT CONSTITUTE A WARRANTY WITH RESPECT TO THE PRODUCTS DESCRIBED HEREIN, AND QORVO HEREBY DISCLAIMS ANY AND ALL WARRANTIES WITH RESPECT TO SUCH PRODUCTS WHETHER EXPRESS OR IMPLIED BY LAW, COURSE OF DEALING, COURSE OF PERFORMANCE, USAGE OF TRADE OR OTHERWISE, INCLUDING THE IMPLIED WARRANTIES OF MERCHANTABILITY AND FITNESS FOR A PARTICULAR PURPOSE. Without limiting the generality of the foregoing, Qorvo products are not warranted or authorized for use as critical components in medical, life-saving, or life-sustaining applications, or other applications where a failure would reasonably be expected to cause severe personal injury or death.